Journal of Sound and Vibration (2000) **234**(2), 207–223
doi:10.1006/jsvi.1999.2886, available online at http://www.idealibrary.com on IDEAL®

SCALE MODELLING OF RAILWAY NOISE BARRIERS

D. C. HOTHERSALL, K. V. HOROSHENKOV, P. A. MORGAN AND M. J. SWIFT

Department Civil & Environmental Engineering, University of Bradford, Bradford, BD7 1DP, England

(*Received* 26 *July* 1999, *and in final form* 16 *November* 1999)

Experiments were carried out in an anechoic chamber using a 1:20 scale model of a high-speed train to determine the insertion loss of various forms of track-side noise barrier. All the barriers investigated had the upper edge level with the bottom of the train windows and were positioned as close as possible to the train, within the limitations of the structure gauge. They thus provided attenuation of noise from sources in the lower portion of the train, in the region of the rails and wheels. The measured performance of plane screens with rigid and sound-absorbing surfaces is compared with values predicted by standard prediction methods for railway noise and the results of a numerical model. The effect of barrier shape and absorptive surfaces upon screening performance is investigated. Results are presented in terms of the insertion loss of the peak SPL of the pass-by profile for a single bogie noise source and for the whole train, and also insertion loss based on $L_{Aeq,1\,h}$. Results for these three measures show similar trends. For the conditions tested insertion loss values for all the screens were lower when the ground behind the barrier was absorbing than when the ground was rigid. The relative changes in insertion loss for the different forms of barrier were similar for the two ground types. Insertion loss values for rigid screens were between 6 and 10 dB lower than those for similar screens with complete sound absorbing surfaces. The application of absorbing areas on rigid screens significantly increases the insertion loss by between 3 and 6 dB. The least efficient screen was a corrugated barrier with a rigid surface. The most efficient screens tested were plane and curved barriers with absorbing surfaces and a multiple edge screen with a part-absorbing surface.

1. INTRODUCTION

Railway noise is increasingly affecting the environment due to the building of new rail links which pass through urban and rural areas and the increasing use of high-speed trains. Noise barriers are commonly used to alleviate the problem particularly in Japan and continental Europe. A range of experimental and theoretical studies has been reported on the efficiency of plane screens and other forms of noise barrier in attenuating railway noise [1–5].

In this paper, a study is presented of the performance of various forms of track-side noise barrier, determined using scale-model experiments conducted in an anechoic chamber. The measured performance of plane screens with rigid and sound-absorbing surfaces is compared with values predicted by standard prediction methods for railway noise and the results of a numerical model. Using models of rolling stock representative of high-speed trains, experiments have been conducted to establish the effect of the barrier shape and absorptive surfaces upon screening performance. The position of the barriers relative to the track has been chosen using an appropriate structure gauge. Results are presented in terms of the insertion loss of the peak SPL of the pass-by profile for a single-bogie noise source and for the whole train, and also insertion loss based on $L_{Aeq,1\,h}$ values, calculated from the measurements.

0022-460X/00/270207 + 17 $35.00/0

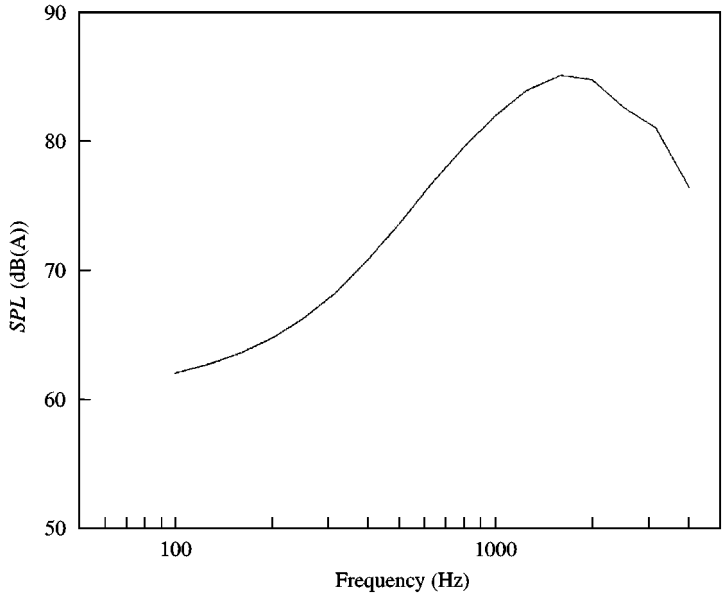

Figure 1. A-weighted third octave band spectrum typical of a TGV-Atlantique train pass-by at a speed of 300 km/h, measured at 25 m from the track [16].

2. SELECTION OF SOURCE CHARACTERISTICS

The main sources of railway noise are the power unit, aerodynamic effects and rail–wheel interaction, see e.g., reference [6]. Attempts have been made to identify the location, strength and spectral content of these sources using various methods [7–11].

For high-speed trains, which are of primary concern, the power units are located typically at the ends of the train. Noise from electric power units is dominated by noise from blowers and the level and spatial distribution of this source depends on the specific type design of the power unit. The contribution from this source to the average energy level for a high-speed train pass-by is small. Consequently, noise generated from the power units is not considered in this study. Aerodynamic noise can be generated from various sources [12] and its contribution is dictated by the speed of the train [13, 14]. The distribution of the sources is dependent on the specific design of the surface profile of the rolling stock. At high speeds, aerodynamic noise resulting from the pantograph and wheel/rail noise on the power cars have been shown to be similar [7]. The sound propagating from the aerodynamic sources on the upper half of the train body and also the locomotive exhaust outlets will be unobstructed by a typical low barrier of approximately 2 m in height. The direct propagation of sound from these sources should be considered separately. Barriers of 5–6 m in height would be required to shield the surroundings from these sources.

Rail–wheel noise can be considered generic to tracked transport systems, although there are subgroupings depending upon the braking system, the rail and wheel construction and the degree of roughness of these elements. In the region of the rails and wheels noise arising from the vibration and interaction of these elements is significantly shielded by low barriers. The purpose of this investigation is to examine the attenuation of noise produced in this region, by using a source located in the bogie units of the train.

A comparison of some published spectra for noise emission from trains has been given in reference [15]. The spectrum adopted in this work is shown in Figure 1 and is derived from site measurements to investigate the performance of noise barrier systems by Houtave [16].

3. DESIGN CRITERIA FOR TRACK-SIDE BARRIERS

Several factors need to be considered in determining the most suitable position and height of a track-side noise barrier. As with all noise barriers, regardless of application, maximum screening efficiency is achieved by locating it as close as possible to the source. However, the proximity to the track is governed by operational safety criteria. The structure gauge defines the envelop of nearest approach of any track-side equipment and for any railway operator may vary according to track speed and type of rolling stock. The possibility of the barriers hindering escape from, or access to, trains in case of emergency must be considered and also the safety of track-side workers.

Barriers attenuation increases with height. The attenuation is minimal if the source is visible from the receiver position. Sources of noise on trains are widely distributed from pantograph to rails so in order to obtain maximum screening potential, barriers that are higher than the train are necessary, possibly also overhanging the track. Low barriers only provide screening from noise generated in the vicinity of the wheels and rails. To provide emergency escape or access and to allow passengers an unrestricted view, a height equivalent to the lower edge of the train windows is commonly selected.

4. EXPERIMENTAL METHOD

4.1. ANECHOIC CHAMBER

The experiments presented in this study were performed in a purpose-built anechoic chamber. The working area inside the chamber was approximately 6 m × 3 m × 3 m and the air temperature was monitored. The humidity within the chamber was controlled at approximately 2·5% RH, ensuring that the air absorption inside the chamber at the model frequency was close to that which would be expected at the full-scale frequency under normal air conditions (50% RH). Compensation for this effect is possible by processing the spectrum of the signal when a single predominant sound path can be defined. However, if it is the intention to model accurately a sound field with multiple sound paths arising from reflection and diffraction effects, as in this case, dehumidification provides the best solution.

4.2. SOURCE AND DETECTOR

The sound source comprised two cylindrical cavities, 20 mm in diameter and 40 mm in depth. Air was admitted into each cavity at a pressure of 10 bar through an aperture 2·5 mm in diameter. The sources were mounted in either the front bogie position of the locomotive (Figure 2) or the bogie of a carriage near the centre of the train. The emission characteristics are shown in Figure 3(a) for the one-third octave bands at 5, 10, 20, 40 and 80 kHz in the plane though the axes of the cylinders, which was the horizontal plane in the model. Similar results are also given in the vertical plane in Figure 3(b) with positive angles in the upward direction. The sources are approximately omni-directional. A number of investigations of the directivity of rail–wheel noise sources have been carried out, with a wide range of results. Monopole and dipole directivity has been reported, and combinations of these distributions. The model sources provided a signal-to-noise ratio of at least 10 dB above the background level in all narrow frequency bands in the chamber for all the measurements.

The sound was detected by a 1/8″ Bruel & Kjaer microphone which was maintained in the same orientation for all measurements. The position of the microphone was controlled remotely by a computer-operated positioning system.

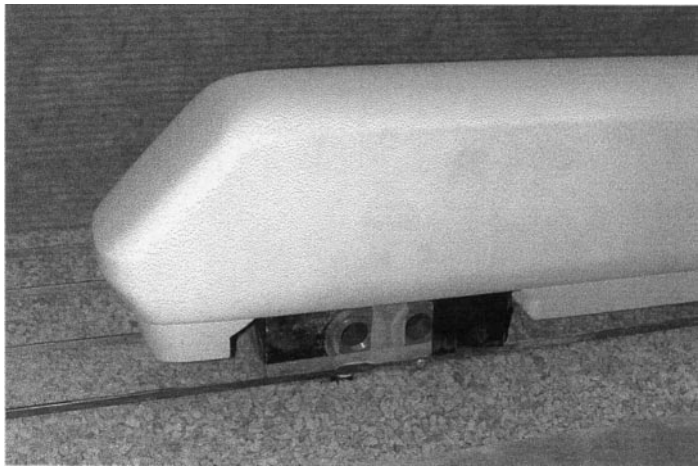

Figure 2. Two cavity air-jet sources mounted in the front bogie of the model locomotive.

4.3. SCALE MODEL

The model used in the experiments was scaled at 1 : 20 (the scaling factor, $m = 20$). Therefore, the full-scale frequency range 50 Hz – 4 kHz relates to 1–80 kHz in the model. Rigid and grassland surfaces were investigated. A polished aluminium surface was used to simulate rigid ground and specially manufactured porous plastic plates, 8 mm in thickness were used to simulate grassland. The flow resistivity of the material deduced from excess attenuation measurements was 2·2 MPa s/m^2 which corresponds to a full-scale flow resistivity of 110 kPa s/m^2 [17]. Track ballast was simulated using gravel. The size of the stones was scaled at $d_1\sqrt{m}$ where d_1 is the full-scale linear dimension of the ballast.

Figure 4(a) shows the cross-section of railway modelled in the chamber. The limit of the structure gauge corresponds to the closest position for overhead catenary masts in the U.K. as specified by the Railtrack Standard Structure Gauge [18]. In the case of plane vertical barriers, their position was fixed by this structure gauge limit. All other barriers were positioned such that the edge closest to the track did not cross the structure gauge limit. The top edges of the vertical barriers and those inclined towards the track were all coincident. In every case, the maximum permissible barrier height corresponded to the lower edge of the carriage window, being 2·75 m above the ground level. Experiments were performed with the rolling stock on the track nearest to the barrier.

Accurate models of British Rail Mk IV carriages and a Class 91 locomotive were used in the experiments. In the U.K., Inter-City 225 trains comprised such rolling stock. The cross-sectional shape of these vehicles is quite similar to that of many other high-speed trains [15]. The experiments were conducted using two different train configurations. The first was composed of four carriages, with the source mounted in the front bogie of the rear carriage. The second configuration was composed of the locomotive and the first half-carriage, with the source mounted in the front bogie of the locomotive (Figure 2). These were designed to characterize how the SPL from a single bogie source changed with distance parallel to the track (i) when the train was present and (ii) on approach and departure of the train. These two conditions must be considered separately when noise barriers are present since in the first case there will be multiple reflections between the side of the train and the noise barrier. This effect will not occur in the second case.

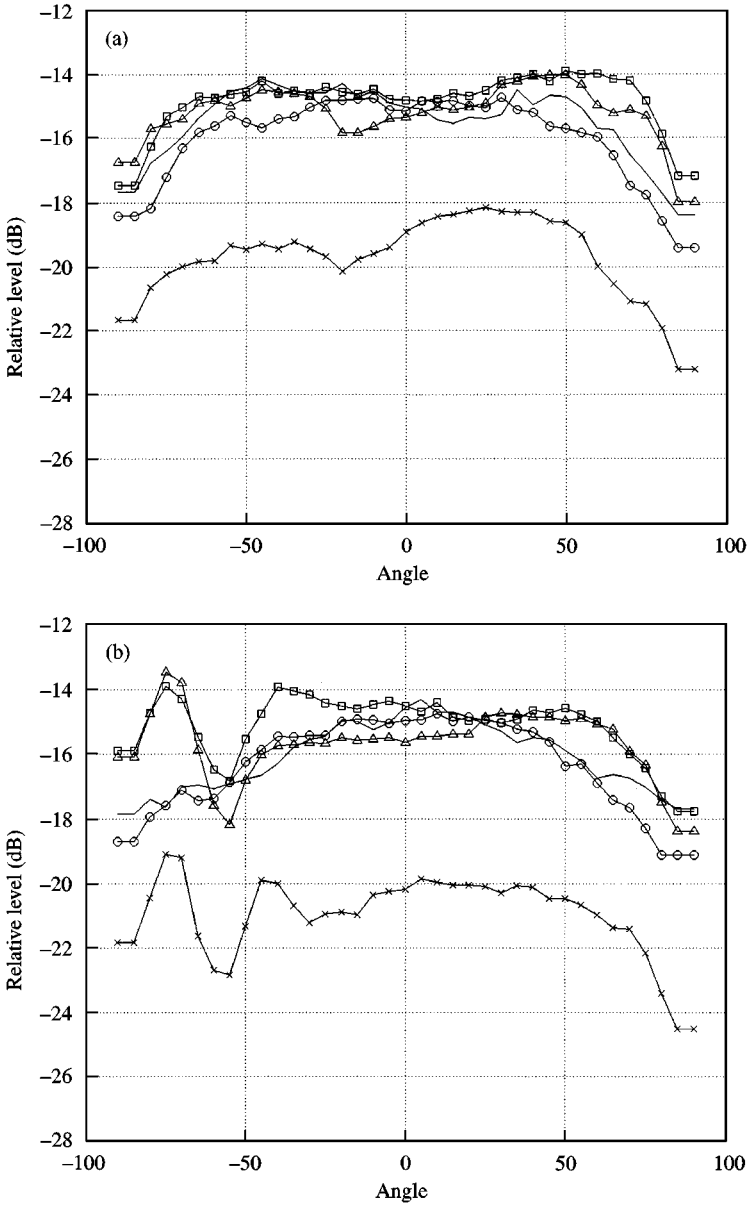

Figure 3. Third-octave band emission characteristics for the source in Figure 2, (a) in the horizontal plane and (b) in the vertical plane. The zero angle is in the direction of the axes of the source cylinders. (——) 5 kHz; (—○—) 10 kHz; (—□—) 20 kHz; (—△—) 40 kHz; (—×—) 80 kHz.

4.4. BARRIER CONFIGURATIONS

The barriers used in the experiments were fabricated either from perspex, plastic or steel. The basic forms are shown in Figure 4. These are (all dimensions at full scale):

(a) A plane vertical screen
(b) A plane vertical screen with the top 0·5 m inclined at an angle of 30° towards the track.

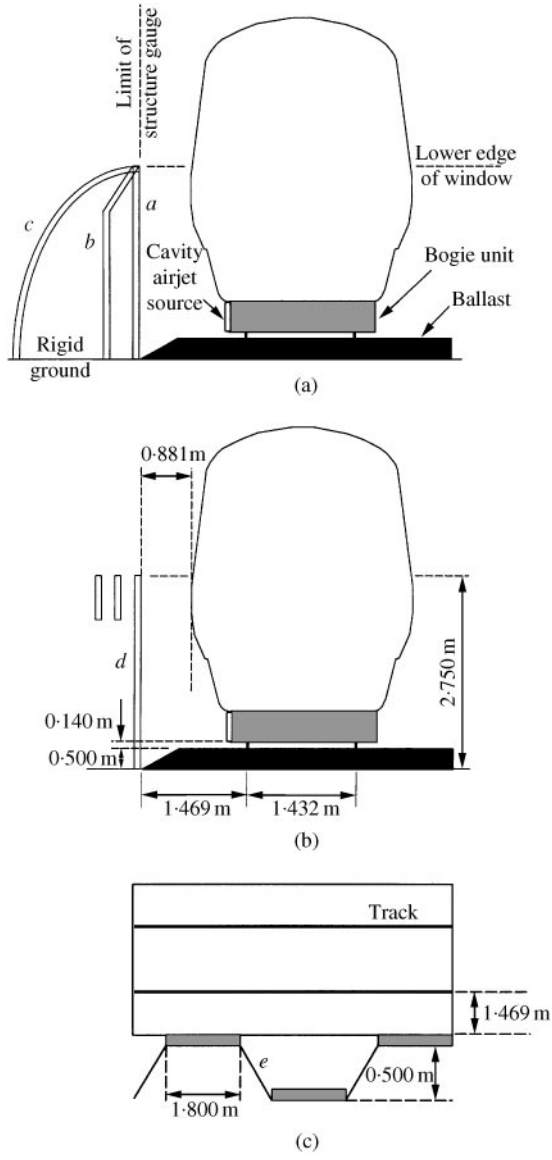

Figure 4. Configuration of the model. (a) and (b) are cross-sections and (c) is a plan, showing the positions of the barriers described in section 4.4.

(c) A curved screen of arc radius 3·25 m inclined towards the track with the tangent to the base normal to the round.
(d) A plane vertical screen fitted with two parallel vertical panels, 0·5 m deep, with a separation of 0·5 m, providing two additional diffracting edges at the same height as the top edge of the main barrier. Figure 4(b) [19].
(e) A barrier comprising vertical panels of constant height with a corrugated plan shape, Figure 4(c).

The barriers were installed parallel to the track. They were tested with rigid surfaces and with absorbing surfaces as described in Table 1. The absorbing surfaces were modelled

TABLE 1

Values of the constants in equation (2) *Examples of fitted curves using the constants are shown in Figures* 5 *and* 6

Barrier type	Receiver height (m)	Coaches		Locomotive	
		c_1	c_2	c_1	c_2
(a) For rigid ground					
No barier	1·5	90·5	24·6	90·3	23·3
	4·5	89·6	18·5	89·9	22·3
Plane screen, rigid	1·5	74·4	14·6	74·2	20·3
	4·5	76·1	15·8	75·7	23·2
Plane screen, top 0·8 m absorbing	1·5	70·0	17·6	70·9	22·1
	4·5	71·7	21·8	72·3	25·6
Plane screen, fully absorbing	1·5	65·5	18·7	65·3	22·9
	4·5	66·6	20·0	65·9	22·4
Multi-edge screen, rigid	1·5	70·7	11·4	70·4	18·2
	4·5	74·7	16·9	74·0	25·3
Multi-edge screen, top 0·5 m absorbing	1·5	64·8	13·9	65·7	19·1
	4·5	66·8	19·0	68·0	24·4
Cranked screen, rigid	1·5	74·3	13·0	74·4	21·6
	4·5	75·4	14·5	75·7	24·6
Cranked screen, top 0·5 m absorbing	1·5	71·2	14·1	72·9	26·1
	4·5	72·4	15·3	74·1	27·6
Curved screen, rigid	1·5	69·4	10·3	69·4	15·8
	4·5	70·3	11·2	70·1	16·0
Curved screen, fully absorbing	1·5	66·6	16·8	66·8	18·0
	4·5	67·2	17·7	67·6	19·4
Corrugated screen, rigid	1·5	76·0	19·9	75·4	21·1
	4·5	77·7	20·5	77·0	22·4
Corrugated screen, part absorbing	1·5	68·6	13·1	69·0	15·9
	4·5	69·5	12·7	69·8	14·9
(b) For grassland					
No barrier	1·5	86·2	31·7	86·1	33·0
	4·5	89·7	19·7	90·5	20·9
Plane screen, rigid	1·5	72·6	14·2	72·3	21·1
	4·5	75·6	17·4	75·2	26·5
Plane screen, top 0·8 m absorbing	1·5	68·7	20·5	69·6	25·7
	4·5	71·3	24·6	72·3	30·5
Plane screen, fully absorbing	1·5	63·8	19·9	64·6	23·0
	4·5	65·7	22·3	66·3	24·5
Multi-edge screen, rigid	1·5	69·2	12·0	69·1	20·1
	4·5	73·7	17·5	73·5	28·4
Multi-edge screen, top 0·5 m absorbing	1·5	63·6	17·0	64·1	21·7
	4·5	66·2	20·8	66·5	24·4
Cranked screen, rigid	1·5	71·7	11·6	72·4	23·2
	4·5	74·2	14·6	74·8	27·6
Cranked screen, top 0·5 m absorbing	1·5	69·3	15·2	70·3	24·7
	4·5	71·5	17·0	72·6	28·1
Curved screen, rigid	1·5	67·0	14·7	67·4	18·3
	4·5	68·4	13·9	69·2	20·1
Curved screen, fully absorbing	1·5	64·7	18·9	65·0	20·7
	4·5	66·1	19·3	66·3	20·7
Corrugated screen, rigid	1·5	73·8	18·9	73·2	19·5
	4·5	76·9	21·0	75·9	22·3
Corrugated screen, part absorbing	1·5	66·4	13·5	66·9	16·3
	4·5	68·1	12·9	68·1	15·1

using a layer of felt that had sound absorbing properties similar to a 190 mm of *Dumex* absorbing system at full scale [17, 20].

4.5. MEASUREMENT PROCEDURE

The signal generated by the source was sampled 64 times at a given receiver position, for a duration of 4 ms, at a sample rate of 4 μs, using the detector microphone connected to an anti-aliasing filter. A DFT of each sample was then calculated between 0 and 100 kHz. The broadband sound pressure level was then calculated using the formula

$$SPL = 10\log_{10}\left[\frac{1}{P_0^2}\sum_{i=1}^{N} h^2(f_i, D)\left(\frac{D}{md}\right)^2\left\{\int_{mf_{il}}^{mf_{iu}} \frac{|g(\tilde{f}, d)|^2}{|g_0(\tilde{f}, d_0)|^2}\left(\frac{d}{d_0}\right)^2 \mathrm{d}\tilde{f}\right\}\right], \tag{1}$$

where $g(\tilde{f}, d)$ is the mean narrowband pressure spectrum at the receiver, proportional to the microphone voltage, at a distance d from the source and at model frequencies $\tilde{f}$. $g_0(\tilde{f}, d_0)$ is the mean reference narrowband pressure spectrum at a distance d_0 from the source in the same azimuth as for $g(\tilde{f}, d)$, in the ground. The reference spectrum is measured in the absence of any noise control elements and is required to normalize the measured levels. $h(f_i, D)$ is the peak pressure spectrum measured in N one-third octave bands for a train pass-by at a distance D from the track at full scale (see Figure 1). f_{iu} and f_{il} are the upper and lower limits of the ith one-third octave band. $(D/md)^2$ is the distance correction applied to the peak pressure spectrum, and p_0 is the reference pressure.

4.6. CALCULATION OF THE INSERTION LOSS

The signal was measured at 25 m (at full scale, here and subsequently) from the near side rail, opposite the active bogie and at intervals along the length of the track for cases (i) and (ii) described in section 4.3. The microphone was situated at approximately 0, 1·5 and 4·5 m above the ground surface. In Figures 5 and 6, the SPL values generated using equation (1) are plotted as a function of distance from the bogie, for a representative selection of the results. The reduction of the SPL with distance is approximately logarithmic and the dotted lines represent curves of the form

$$SPL = c_1 + c_2\log_{10}\left(\frac{25}{d}\right) \quad \text{dB (A)} \tag{2}$$

fitted to the data. This procedure has been repeated for all cases and the values of c_1 and c_2 are given in Table 1.

As expected, for the cases where no barrier is present the decay rates with distance, represented by the constant c_2, are similar for cases (i) and (ii). For rigid ground the values are near 20 which corresponds to point source attenuation of 6 dB/doubling of distance. For grassland the attenuation constant is approximately 32 for the lower receiver positions, reducing to approximately 20 at a height of 4·5 m where the ground attenuation effect is expected to be small.

Results for rigid and absorbing plane screens are also shown in Figures 5 and 6. In this case for rigid ground the attenuation constant remains close to 20 for propagation beyond the ends of the train (case (ii)) and there is a reduction in the attenuation rate when the carriages are present. In this case the constant is approximately 15. Similar trends are

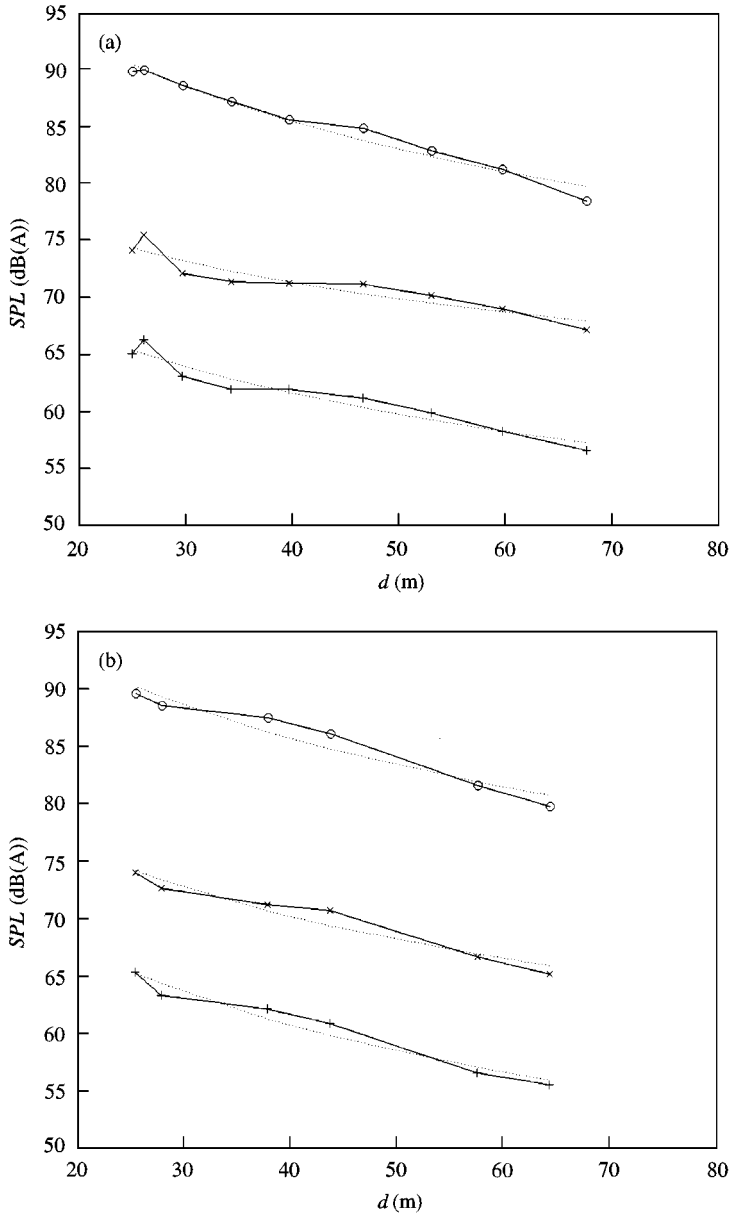

Figure 5. Sound pressure level as a function of distance over rigid ground from a single bogie source, d. The receiver height is 1·5 m. (a) is for propagation along the train (case (i)) and (b) is for propagation beyond the ends of the train (case (ii)). Points indicate measured data, (○) free field, (×) plane rigid screen, (+) plane-absorbing screen. Dotted lines are fitted curves calculated using the constants in Table 1.

observed for absorbing ground. For the case of the absorbing plane screen the attenuation rate for case (ii) is close to 20 since the multiple reflection effects between the train and the barrier which enhance propagation are reduced.

The c_1 values for case (i) are the fitted peak pass-by SPLs for the single bogie and they can be used to determine the insertion loss. These results are given in Table 2.

By setting up a given train configuration (say eight carriages) it is possible to identify all the bogie positions and to generate a pass-by profile for a specific single bogie which extends

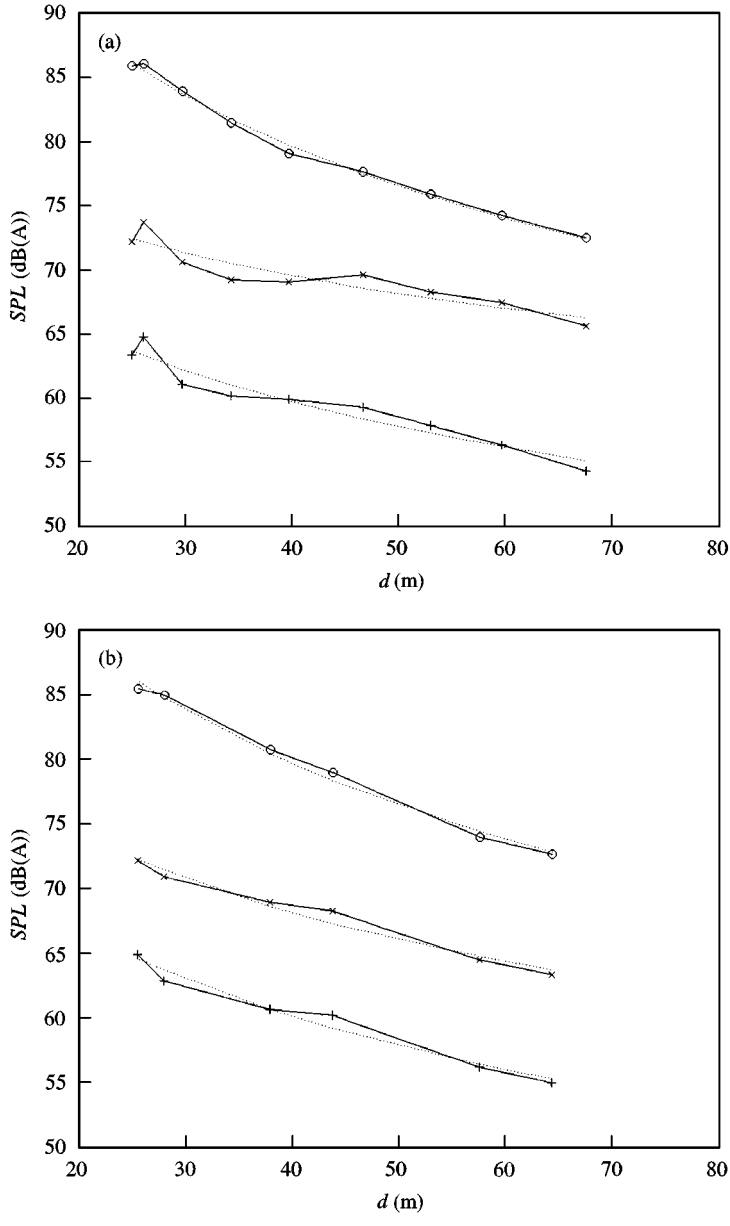

Figure 6. Sound pressure level as a function of distance over grassland from a single bogie source, d. (a) is for propagation along the train (case (i)) and (b) is for propagation beyond the ends of the train (case (ii)). Points indicate measured data, (○) free field, (×) plane rigid screen, (+) plane-absorbing screen. Dotted lines are fitted curves calculated using the constants in Table 1.

beyond the ends of the train. When this condition applies the decay rates from case (ii) are used. Combining these profiles for each of the bogies the pass-by profile for a complete train can be generated. Examples are shown in Figure 7 as a function of time for a train speed of 200 km/h. These have some similarity to pass-by profiles measured in the field, but differ in two ways. The increase in level sometimes associated with the passage of the power unit does not occur. Also the sharp rise and slower decay of the SPL as the train passes is not

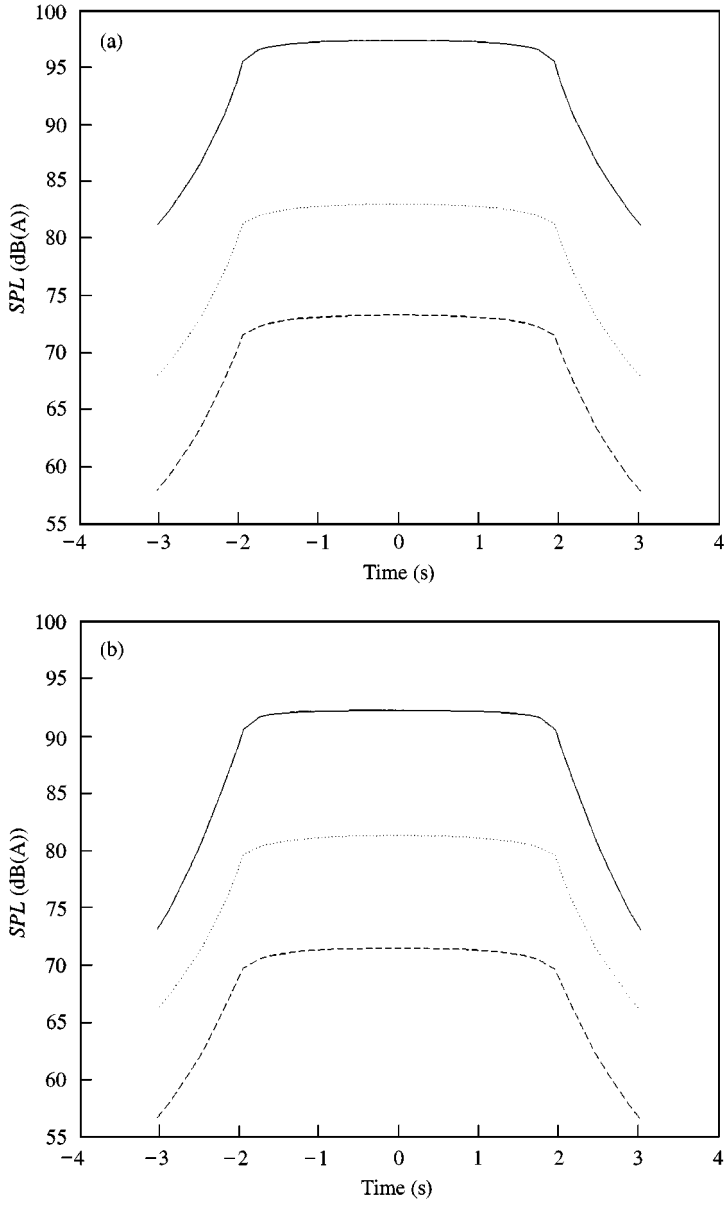

Figure 7. Train pass-by profiles for a 225 train travelling at 200 km/h. The reception point is 25 m from the near-side rail and 1·5 m above ground. (a) rigid ground (b) grassland. Solid line is for free field. Dotted line is for a rigid plane screen. Dashed line is for an absorbing plane screen.

simulated. Asymmetry can be generated by making allowance for the approach and departure velocity of the train but Makarewicz and Yoshida [21] primarily attribute the effect to air turbulence. The insertion loss in the peak SPL of the train pass-by profile can be calculated for each barrier and the results are indicated in Table 2.

Integration of the pass-by profile enables the total energy to be calculated and this can be expressed as the $L_{Aeq,\,1\,\mathrm{h}}$. The insertion loss calculated from these results is also shown in Table 2.

TABLE 2

Insertion loss for different forms of noise screen. The receiver position is at 25 m *from the near-side track and at the heights indicated. Results are for rigid and absorbing ground between the barrier and receiver*

	Insertion loss (dB)					
	Rigid ground			Absorbing ground		
Barrier type	0·0 m	1·5 m	4·5 m	0·0 m	1·5 m	4·5 m
Free field (SPLs)						
Bogie	92·4	90·5	89·6	79·7	86·2	89·7
Pass-by	100·1	97·4	97·6	85·5	92·3	97·4
$L_{Aeq,\,1\,h}$	70·6	67·9	68·0	56·1	62·8	67·9
Plane screen, rigid						
Bogie	15·9	16·1	13·5	8·0	13·6	14·1
Pass-by	14·8	14·3	12·9	6·0	10·9	13·7
$L_{Aeq,\,1\,h}$	14·8	14·3	13·0	6·1	10·9	13·8
Plane screen, top 0·8 m absorbing						
Bogie	20·2	20·5	17·9	11·7	17·5	18·4
Pass-by	20·1	19·3	18·5	10·5	16·0	19·2
$L_{Aeq,\,1\,h}$	20·1	19·2	18·4	10·5	16·0	19·1
Plane screen, fully absorbing						
Bogie	24·7	25·0	23·1	16·6	22·4	23·9
Pass-by	24·5	24·0	23·3	15·0	20·7	24·4
$L_{Aeq,\,1\,h}$	24·5	24·0	23·3	15·0	20·7	24·3
Multi-edge screen, rigid						
Bogie	19·7	19·8	14·9	11·3	17·1	16·0
Pass-by	17·9	17·2	14·6	8·3	13·8	15·6
$L_{Aeq,\,1\,h}$	17·8	17·2	14·6	8·4	13·8	15·7
Multi-edge screen, top 0·5 m absorbing						
Bogie	25·8	25·7	22·8	16·7	22·7	23·5
Pass-by	24·9	23·7	22·9	14·1	20·5	23·7
$L_{Aeq,\,1\,h}$	24·8	23·7	22·8	14·1	20·5	23·7
Cranked screen, rigid						
Bogie	16·3	16·2	14·2	8·6	14·5	15·4
Pass-by	14·6	14·0	13·4	6·7	11·1	14·4
$L_{Aeq,\,1\,h}$	14·5	14·1	13·4	6·7	11·1	14·5
Cranked screen, top 0·5 m absorbing						
Bogie	19·3	19·3	17·3	11·8	17·0	18·2
Pass-by	18·0	17·3	16·6	9·6	14·4	17·7
$L_{Aeq,\,1\,h}$	17·9	17·3	16·6	9·7	14·4	17·7
Curved screen, rigid						
Bogie	21·1	21·1	19·3	13·1	19·2	21·2
Pass-by	18·7	18·3	17·8	10·8	16·5	20·0
$L_{Aeq,\,1\,h}$	18·5	17·1	17·6	10·8	16·5	20·0
Curved screen, fully absorbing						
Bogie	24·0	23·9	22·4	15·4	21·6	23·6
Pass-by	22·6	22·5	22·2	14·1	19·8	23·5
$L_{Aeq,\,1\,h}$	22·4	22·5	22·1	14·1	19·7	23·5
Corrugated screen, rigid						
Bogie	14·2	14·4	11·9	7·0	12·5	12·9
Pass-by	14·2	13·7	12·3	5·6	10·5	13·1
$L_{Aeq,\,1\,h}$	14·2	13·7	12·2	5·7	10·6	13·2
Corrugated screen, part absorbing						
Bogie	22·0	21·9	20·2	13·8	19·9	21·6
Pass-by	20·4	19·7	18·9	11·9	16·9	20·2
$L_{Aeq,\,1\,h}$	20·2	19·7	18·8	11·9	16·9	20·1

TABLE 3

Measured and predicted values for $L_{Aeq,1\,h}$ *and insertion loss at* 25 m *from the near-side rail and* 1·5 m *above ground. Plane screen*

Ground type	Barrier type	$L_{Aeq,1\,h}$ (dB)			Insertion loss (dB)		
		Nordic model	CRN	Measured	Nordic model	CRN	Measured
Rigid	None	64·0	61·3	68·1	—	—	—
	Rigid	53·7	47·6	53·6	10·3	13·7	14·3
	Absorbing	48·0	43·0	43·9	16·0	18·3	24·0
Absorbing	None	61·6	61·3	62·8	—	—	—
	Rigid	42·3	47·6	51·9	9·3	13·7	10·9
	Absorbing	47·7	43·0	42·1	13·9	18·3	20·7

5. DISCUSSION

5.1. COMPARISON WITH OTHER RESULTS

General prediction methods for noise from railways have been developed in many countries. There are at least nine different models existing over European countries. In the calculation of barrier attenuation a path difference approach is almost universally adopted and plane screens are assumed. The differences between the methods are related to the source location, treatment of the effects of absorbing surfaces, the use of curved or straight sound paths and whether the calculations are carried out for the broadband spectrum or via separate spectral bands. In Table 3, the experimental model results for $L_{Aeq,1\,h}$ from the passage of a single train are shown for propagation above rigid and absorbing ground and in the presence of rigid and absorbing plane screens. Insertion loss values are also given. These can be compared with the predicted values using the Nordic model [22] and the U.K. model the Calculation of Railway Noise (CRN) [23]. The results do not agree well and consistent trends are not easy to identify. The measured insertion losses for the absorbing screen are, however, somewhat greater than those predicted by the two standard methods. The poor agreement may be attributed to difficulties encountered in applying these standard methods to the exact experimental conditions. The minimum distance from track centreline to barrier is 3 m in the Nordic model and the exact train type is not available. In the U.K. model the attenuation attributable to grassland is zero for propagation distances of up to 25 m.

Investigations of the detailed effects of barrier shape and surface cover are uncommon. In this investigation, the upper edges of the different noise barriers are all coincident, with the position chosen according to standard U.K. structure gauge for existing lines. In other studies using the same source spectrum [4, 16, 24] the bases of the barriers are coincident and the proximity to the track set according to different structure gauges. In the present study, the noise barriers are significantly closer to the track than those used in previous work and consequently higher values of insertion loss are observed. However, the relative efficiency of the different forms compares well.

Conditions similar to those used in the present study have been adopted in an investigation using numerical modelling [15]. The train cross-section, the barrier positions and the source spectrum were the same and the ground was absorbing, with the characteristics of grassland. In Table 4, the experimental results for insertion loss in the

TABLE 4

Comparison of insertion loss for various forms of barrier obtained from the experimental model and a numerical model [15]. *The receiver is* 1·5 m *above absorbing ground and* 25 m *from the near-side rail. Note the differences in conditions for the two methods discussed in the text*

	Insertion loss (dB)	
Barrier type	Experimental model	Numerical model
Plane screen, rigid	10·9	13·6
Plane screen, part absorbing	16·0	16·6
Plane screen, absorbing	20·7	19·1
Curved screen, rigid	16·5	14·8
Curved screen, absorbing	19·8	17·8

maximum SPL from a train pass-by are compared with the results of the numerical model. Reasonable agreement is observed. The discrepancies in the results may be attributed to the different source characteristics. In the numerical model the bogie source was represented by a dipole. The numerical model is two-dimensional and the calculated sound field is equivalent to that for a coherent line source along the line of the bogies in three dimensions.

5.2. REPEATABILITY OF THE EXPERIMENTS

Free field measurement were repeated over the period of several months during which the experiments were performed. Results will be quoted at the receiver height of 1·5 m. For the four measurements for propagation above rigid ground the range in the values of c_1 and $L_{Aeq,\,1\,\mathrm{h}}$ were 0·6 and 0·3 dB respectively. For absorbing ground the ranges were 0·4 and 0·1 dB, respectively, over three measurements. When the results of previous experiments using two other types of sound source were also included [25, 26] the range increased to 1·2 and 0·8 dB respectively. For the two measurements carried out with the plane rigid screen on rigid ground the difference in c_1 was 0·9 dB and the difference in $L_{Aeq,\,1\,\mathrm{h}}$ was 0·7 dB. For the other types of screen, comparisons can only be made between results obtained using different sources. A source with approximately dipole emission characteristics produced results for the insertion loss of absorbing screens which were consistently approximately 3 dB lower than for the source described in section 4.2.

5.3. SCREENING PERFORMANCE

Very similar trends are observed between the three different measures of insertion loss described in section 4.6 and shown in Table 2. The results for propagation above rigid and absorbing ground also show consistent trends. For rigid ground there is a progressive, although quite small reduction in insertion loss with height of the receiver. For the absorbing ground the lowest values are close to the ground and these increase by about 5–6 dB at 1·5 m and a further 1–3 dB at 4·5 m. The difference in insertion loss between the rigid and absorbing ground cases is approximately 9, 3 and -1 dB at receiver heights of 0, 1·5 and 4·5 m respectively.

The performance of the rigid screens is consistent for all positions and both ground types. The cranked and corrugated screens have insertion losses similar to the plane screen while

the multiple edge and the curved screens have insertion losses approximately 2–5 dB greater. The improved performance of the multiple edge screen is attributable to the diffraction effects at each of the edges [19]. The curved screen reflects sound towards the ballast, where a proportion of the energy is absorbed.

The effect of introducing absorptive surfaces on to the track-facing side of the barriers is to improve the performance in every case. For the plane screen, the insertion loss rises by about 5 dB when the top 0·8 m is absorbing and by about 10 dB when the whole surface is absorbing. When the upper 0·8 m of the multiple edge screen is absorbing the performance is approximately the same as for the fully absorbing plane screen. The effect of applying absorbent to the upper section of the cranked screen is to improve the insertion loss by only about 3 dB. A similar improvement is observed in the parabolic screen when it is fully absorbing. The application of absorbent to selected surfaces of the corrugated screen (see Figure 4(b)) increases the insertion loss by 6 dB. There is a remarkable consistency in the ultimate insertion loss attainable from the more efficient noise barrier configurations. For example, for $L_{Aeq,\,1\,\mathrm{h}}$ the maximum insertion loss at 1·5 m height is approximately 24 dB for rigid ground and 20 dB for absorbing ground. This applies to the absorbing plane screen, the absorbing parabolic barrier and the part absorbing multiple edge screen. It is clear that the absorbent largely removes the effects of multiple reflection between the barrier and the side of the train. For the configurations considered here the maximum effect of this on the insertion loss is about 10 dB.

6. CONCLUSIONS

Experimental scale modelling is a useful technique for investigating outdoor sound propagation in 3-D. The use of a computer and appropriate software for source activation, microphone positioning and the processing of measured signals allows experiments to be carried out extremely efficiently. The major expense is the construction and installation of the models. Factors which affect the accuracy are the selection of materials to model sound-absorbing surfaces and the emission characteristics of the source. When high values of insertion loss are measured it is important to ensure good sealing of the noise barriers.

The efficiency of railway noise barriers can be expressed in terms of the insertion loss for: (i) the peak SPL for a single bogie source; (ii) the peak SPL during a train pass-by; (iii) the $L_{Aeq,\,1\,\mathrm{h}}$ or L_{AE} for a train pass-by. The insertion loss results for these three measures show similar trends.

All the barriers investigated had the upper edge level with the bottom of the train windows and were positioned as close as possible to the train, within the limitations of the structure gauge. They thus provided attenuation of noise from sources in the lower portion of the train, in the region of the rails and wheels. The sources used in the model were situated at the bogie position.

For the conditions tested insertion loss values for all the screens were lower when the ground behind the barrier was absorbing than when the ground was rigid. The relative changes in insertion loss for the different forms of barrier were remarkably similar for the two ground types. The insertion loss for rigid screens was 6–10 dB lower than for similar screens with complete sound-absorbing surfaces. The application of absorbing areas on rigid screens significantly increases the insertion loss by between 3 and 6 dB. The least efficient screen was a corrugated barrier with a rigid surface. The most efficient screens tested were plane and curved barriers with absorbing surfaces and a multiple edge screen with a partly absorbing surface.

The barrier positions used in this investigation are as close to the track as possible. As the distance to the track increases the insertion loss will decrease. It is likely, however, that for different barrier positions and receiver position to these used here the general trends in the results will remain the same.

ACKNOWLEDGMENTS

The research was supported by grant GR/K73367 from the Engineering and Physical Sciences Research Council. The train models were provided by GEC Alsthom Metro-Cammell. The contribution of Dr S. N. Chandler Wilde to the development of the numerical model is acknowledged.

REFERENCES

1. Y. HIDAKA, H. TACHIBANA, Y. MATSUI and R. KANEKO 1995 *Proceedings of Inter-Noise '95*, Newport Beach, 215–218. Measurement of sound radiation from Shinkansen train by sound intensity method.
2. P. JEAN 1998 *Journal of Sound and Vibration* **212**, 275–294. A variational approach for the study of outdoor sound propagation and application to railway noise.
3. E. RUDOLPHI and L. ÅKERLÖF 1996 *Proceedings of Inter-Noise '96*, Liverpool, 799–802. Full scale tests on the design of railway noise barriers.
4. J.-P. CLAIRBOIS, P. HOUTAVE and N. NICOLAS 1997 *Proceedings of Inter-Noise '97*, Budapest, 425–428. Specific designs of noise barriers for trains. Part II: *in-situ* verification of effectiveness.
5. P. F. VAN TOL 1997 *Proceedings of Inter-Noise '97*, Budapest, 429–432. An array measurement technique applied to high speed train noise barriers.
6. C. STANWORTH 1987 *Transportation Noise Reference Book* (P. M. Nelson, editor). London: Butterworth. Sources of railway noise.
7. G. HOLZL, P. FODIMAN, K.-P. SCHMITZ, M. A. PALLAS and B. BARSIKOW 1994. *Proceedings of Inter-Noise '94*, Yokohama, 193–198. Deufrako-2: localised sound sources on the high-speed vehicles ICE, TGV-A and TR 07.
8. J. D. VAN DER TOORN, H. HENDRIKS and T. C. VAN DEN DOOL 1996 *Journal of Sound and Vibration* **193**, 113–121. Measuring TGV source strength with Syntacan.
9. B. BARSIKOW 1996 *Journal of Sound and Vibration* **193**, 283–293. Experiences with various configurations of microphone arrays used to locate sound sources on railway trains operated by the DB AG.
10. M. KAWAHARA, H. HOTTA, M. HIROE and J. KAKU 1997 *Proceedings of Inter-Noise '97*, Budapest, 151–154. Source identification and prediction of Shinkansen noise by sound intensity.
11. B. BARSIKOW and M. KLEMENZ 1998 *Proceedings of the 16th International Congress on Acoustics, Seattle*, 2229–2230. Diagnosis of noise sources on high-speed trains using the microphone array technique.
12. W. F. KING III 1996 *Journal of Sound and Vibration* **193**, 349–358. A precis of developments in the aeroacoustics of fast trains.
13. W. F. KING III 1977 *Journal of Sound and Vibration* **54**, 361–378. On the role of aerodynamically generated sound in determining the radiated noise levels of high speed trains.
14. B. MAUCLAIRE 1990 *Proceedings of Inter-Noise '90*, Gothenberg, 371–374. Noise generation by high speed trains. New information acquired by SNCF in the field of acoustics owing to the high speed test program.
15. P. A. MORGAN, D. C. HOTHERSALL and S. N. CHANDLER-WILDE 1998 *Journal of Sound and Vibration* **217**, 405–417. Influence of shape and absorbing surface—a numerical study of railway noise barriers.
16. P. HOUTAVE 1997 Private communication. Acoustical Technologies, Brussels, Belgium.
17. K. V. HOROSHENKOV, D. C. HOTHERSALL and K. ATTENBOROUGH 1996. *Journal of Sound and Vibration* **194**, 685–708. Porous materials for scale model experiments in outdoor sound propagation.
18. RAILTRACK 1995 *Railway Group Standard GC/RT* 5204, *Structure Gauging and Clearances.*

19. D. H. CROMBIE, D. C. HOTHERSALL and S. N. CHANDLER-WILDE 1995 *Applied Acoustics* **44**, 353–367. Multiple-edge noise barriers.
20. K. V. HOROSHENKOV, S. J. MERCY, D. C. HOTHERSALL 1999 *Journal of Sound and Vibration* **223**, 795–819. Scale modelling of sound propagation in a city street canyon.
21. R. MAKAREWICZ and M. YOSHIDA 1996 *Applied Acoustics* **49**, 291–306. Railroad noise in an open space.
22. NORDIC COUNCIL OF MINISTERS 1996 *Railway Traffic Noise—The Nordic Prediction Method. TemaNord*. Copenhagen,1996: 524. Nordic Publishing House.
23. DEPARTMENT OF TRANSPORT 1995 *Calculation of Railway Noise*. London: HMSO.
24. P. HOUTAVE and J.-P. CLAIRBOIS 1997 *Proceedings of Inter-Noise '97*, Budapest, 421–424. Specific designs of noise barriers for trains. Part I: theoretical study of forms and materials.
25. D. C. HOTHERSALL, K. V. HOROSHEMKOV and P. A. MORGAN 1998 *Proceedings of The 16th International Congress on Acoustics*. Seattle, 465–466. Scale modelling of railway noise barriers.
26. D. C. HOTHERSALL, K. V. HOROSHENKOV, M. J. SWIFT and P. A. MORGAN 1999 *Proceedings of the Institute of Acoustics* **21**, 35–40, Model investigations of the performance of railway noise barriers.